Eur. Phys. J. D **32**, 261–267 (2005)
DOI: 10.1140/epjd/e2004-00199-6

THE EUROPEAN PHYSICAL JOURNAL D

Test of quantum nonlocality by full collection of polarization entangled photon pairs

M. Barbieri, C. Cinelli, F. De Martini, and P. Mataloni[a]

Dipartimento di Fisica and Istituto Nazionale per la Fisica della Materia, Università di Roma "La Sapienza", 00185 Roma, Italy

Received 13 July 2004 / Received in final form 8 October 2004
Published online 4 January 2005 –

Abstract. We have experimentally tested the nonlocal properties of the states generated by a high brilliance source of entanglement which allows the direct measurement of virtually all the photon pairs emitted over the emission cone at a certain wavelength. By this source we could verify the Hardy's ladder proof about contradiction between quantum mechanics and local realism for 41% of entangled photon pairs. The realization of an experimental test of quantum nonlocality with no need of supplementary assumptions is also extensively discussed.

PACS. 03.65.Ud Entanglement and quantum nonlocality (e.g. EPR paradox, Bell's inequalities, GHZ states, etc.) – 03.67.Mn Entanglement production, characterization and manipulation – 42.65.Lm Parametric down conversion and production of entangled photons

1 Introduction

Since the EPR discovery in 1935 [1] followed by a many decades long debated endeavour ending with the emergence of Bell's inequalities [2,3] and with the first experimental tests [3,4], entanglement, "*the characteristic trait of quantum mechanics*" [5], has represented the irrevocable signature of quantum nonlocality. In recent years the violation of these inequalities has been successfully tested many times by optical experiments, mostly involving polarization entangled photons generated by Spontaneous Parametric Down Conversion (SPDC) in a nonlinear (NL) crystal. In addition, a further nonlocality test not involving inequalities was proposed years ago by Lucien Hardy (Hardy's ladder theorem) [6] and soon realized experimentally by a SPDC process [7].

In this paper we report yet another nonlocality test, performed either by the standard Bell configuration or by Hardy's no-inequality "ladder" scheme. The novelty of this experiment consists of the peculiar spatial properties of the output **k**-vector distribution generated by the SPDC source adopted in this experiment [8,9]. This source allows in principle, to couple to the output detectors the full set of optical modes carrying the particle pairs involved in the EPR measurement. In other words, all entangled pairs created over the entire set of wavevectors allowed by phase matching can virtually be detected. Since the detected emission process is entirely "quantum", i.e. not affected by any "classical" manipulation, such as wavelength (wl) and wavevector (wv) filtering, this scheme allows in principle the realization of the necessary premises underlying the original formulation of the EPR Paradox.

The work is organized as follows: in Section 2 a short review of Hardy's ladder theorem is presented. Section 3 concerns the description of the parametric source. The high quality of the realized output entangled state and the experimental verification of Hardy's ladder theory up to the 20th step are presented in Section 4. Finally, we discuss in Section 5 about the possibility of realizing by this source an experimental test of quantum nonlocality with no need of supplementary assumptions [10,11].

2 Hardy's ladder theorem

Let's outline here Hardy's "ladder" theory [6,7]. Consider a polarization entangled state of the form:

$$|\Phi\rangle = \alpha\,|H_A H_B\rangle - \beta\,|V_A V_B\rangle\,, \tag{1}$$

where α and β are real constants, $\alpha \neq \beta$, $\alpha^2 + \beta^2 = 1$. On photon A (B) polarization measurements are made along one of $K+1$ possible direction A_k, $k = 0, ..., K$. The corresponding quantum states are $|A_k\rangle$ and $|B_k\rangle$ with orthogonal states $\left|A_k^{\perp}\right\rangle$ and $\left|B_k^{\perp}\right\rangle$. Their explicit expression are

$$|H_A\rangle = c_k\,|A_k\rangle + c_k^{\perp}\left|A_k^{\perp}\right\rangle, \tag{2}$$

$$|V_A\rangle = c_k^{\perp}\,|A_k\rangle - c_k\left|A_k^{\perp}\right\rangle, \tag{3}$$

$$|H_B\rangle = c_k\,|B_k\rangle + c_k^{\perp}\left|B_k^{\perp}\right\rangle, \tag{4}$$

$$|V_B\rangle = c_k^{\perp}\,|B_k\rangle - c_k\left|B_k^{\perp}\right\rangle, \tag{5}$$

[a] e-mail: paolo.mataloni@uniroma1.it

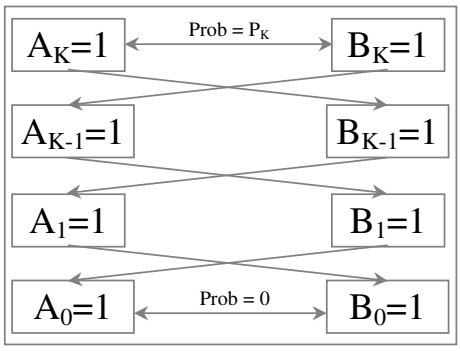

Fig. 1. Representation of the ladder contradiction.

where we have chosen real values of c_k and $c_k^{\perp}$, i.e. $|A_k\rangle$, $|B_k\rangle$ correspond to linear polarizations.

These directions are chosen in order to satisfy the following properties:

$$P_K = \mathrm{Prob}(A_K = 1, B_K = 1) \neq 0, \quad (6)$$

$$\mathrm{Prob}(A_k = 1, B_{k-1} = 0) = 0 \text{ for } k = 1 \text{ to } K, \quad (7)$$

$$\mathrm{Prob}(A_{k-1} = 0, B_k = 1) = 0 \text{ for } k = 1 \text{ to } K, \quad (8)$$

$$\mathrm{Prob}(A_0 = 1, B_0 = 1) = 0. \quad (9)$$

We label by $A_k = 1$ and $A_k = 0$ the event in which A_k is measured with outcomes A_k and $A_k^{\perp}$, respectively.

It can be shown that these requirements are mutually inconsistent in the framework of local realism. Let's refer to the scheme shown in Figure 1 and consider for simplicity the case $K = 2$. Suppose that in one run of the experiment A_2 and B_2 have been measured with results $A_2 = 1$ and $B_2 = 1$. By assuming local realism we have to assign to any possible direction A_k and B_k a certain value 0 or 1, because any property of the state is determined by a proper set of hidden variables. On the other hand quantum mechanics does not require certain predictions, since generally different measurements A_k and $A_{k'}$ do not commute. Having measured $A_2 = 1$ it comes out from (7) that if we had measured B_1, we would have certainly found $B_1 = 1$. Similarly, $B_2 = 1$ implies $A_1 = 1$. This allows us to go down a rung down the ladder (Fig. 1). We may follow the same argument and obtain the result that $A_0 = 1$ and $B_0 = 1$ can be measured simultaneously at least with probability P_K, in contradiction with prediction (9). This result demonstrates that nonlocality resides into the logical basis of quantum mechanics. The same logical procedure can be applied to the cases $K > 2$.

An explicit construction of states $|A_k\rangle$ and $|B_k\rangle$ which satisfy Hardy's requirements is given by starting from equation (9)

$$\langle A_0 B_0 | \Phi \rangle = 0. \quad (10)$$

It implies:

$$c_0 \propto \beta^{1/2}, \; c_0^{\perp} \propto \alpha^{1/2}. \quad (11)$$

By equations (7, 8) we have:

$$\left\langle A_k B_{k-1}^{\perp} | \Phi \right\rangle = 0, \quad (12)$$

$$\left\langle A_{k-1}^{\perp} B_k | \Phi \right\rangle = 0. \quad (13)$$

By combining the last two equations together with (11), we find:

$$c_k \propto (-1)^k \beta^{k+1/2}, \; c_k^{\perp} \propto \alpha^{k+1/2}. \quad (14)$$

The latter equation allows us to evaluate the probability P_K,

$$P_K = |\langle A_K B_K | \Phi \rangle|^2 = \left(\frac{\alpha\beta^{2K+1} - \beta\alpha^{2K+1}}{\beta^{2K+1} + \alpha^{2K+1}} \right)^2, \quad (15)$$

$$P_K = \frac{1}{(1+\gamma^2)} \left(\frac{\gamma - \gamma^{2K+1}}{1 + \gamma^{2K+1}} \right)^2, \quad (16)$$

with $\gamma = \alpha/\beta$ representing the degree of entanglement. For any K a particular value of γ, which maximizes P_K, exists. We can associate the polarization angle θ_k, to any event A_k and B_k, hence we can write:

$$|A(\theta_k)\rangle = \cos\theta_k \, |H\rangle + \sin\theta_k \, |V\rangle \, . \quad (17)$$

By applying (14), it is found:

$$\tan\theta_k = (-1)^k \gamma^{k+1/2}. \quad (18)$$

For $K = 1$, the maximum value of P_K is 0.09, corresponding to $\gamma = 0.46$. The asymptotic value of P_K is $P_K = 0.5$ in the limit $K \to \infty$. It comes out that no contradiction with local realism can be observed with maximally entangled states, where $P_K = 0$ for $\alpha = \beta = 1/\sqrt{2}$.

Hardy's ladder theorem demonstrates a purely logical contradiction between quantum mechanics and local realism without involving inequalities. However, inequalities are necessary as quantitative test in a real experiment in order to avoid the conceptual difficulties of a nullum experiment. A proper inequality can be derived by combing Hardy's requirements (6, 7, 8, 9) with Clauser-Horne inequalities, which, in this case, can be written as [3]

$$\mathrm{Prob}(A_k = 1, B_k = 1) - \mathrm{Prob}(A_{k-1} = 1, B_{k-1} = 1) \leq \mathrm{Prob}(A_k = 1, B_{k-1} = 0) + \mathrm{Prob}(A_{k-1} = 0, B_k = 1). \quad (19)$$

By summing these inequalities over $k = 1$ to K, we obtain:

$$P_K \leq \mathrm{Prob}(A_0 = 1, B_0 = 1) + \sum_{k=1}^{K} [\mathrm{Prob}(A_k = 1, B_{k-1} = 0) + \mathrm{Prob}(A_{k-1} = 0, B_k = 1)]. \quad (20)$$

Since the right term is equal to zero, this inequality is violated by quantum mechanical predictions by an amount equal to P_K.

3 The parametric source

The active element of the source of polarization-entangled photons is a type-I, 0.5 mm thick, β-barium-borate (BBO) crystal, which is excited in two opposite directions,

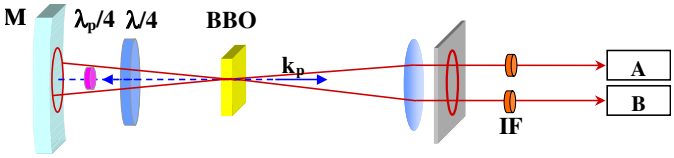

Fig. 2. Layout of the high brilliance source of polarization entanglement.

$\mathbf{k}_p$ and $-\mathbf{k}_p$ by a slightly focused vertically (V) polarized cw Ar^+ laser UV pump beam ($\lambda_p = 363.8$ nm). This is back-reflected by a spherical mirror (M) with curvature radius R, at a distance $d = R$ from the BBO (Fig. 2). Each of the two independent SPDC processes generates two correlated photons with wavelengths λ_i, ($i = A, B$), and common H polarization, corresponding to the product state $|H_A H_B\rangle$. They are emitted with equal probability over symmetric wavevectors belonging to the surfaces of two circular cones with axis $\mathbf{k}_p$ and $-\mathbf{k}_p$ and semi-aperture $\xi \simeq 2.9°$. In this experiment degenerate pairs are selected: $\lambda_A = \lambda_B = \lambda = 2\lambda_p = 727.6$ nm. The two cones overlap into a single one with axis $\mathbf{k}_p$, i.e. directed towards the right hand side (r.h.s.) of Figure 2, by back-reflection over M of the radiation cone with axis $-\mathbf{k}_p$. If in the round trip BBO-M-BBO the polarization of the emitted pairs belonging to the l.h.s. cone is flipped, i.e. $H_i \rightarrow V_i$, by double passage through a zero-order $\lambda/4$ waveplate (wp), the generated pure entangled state is

$$|\Phi\rangle = \frac{1}{\sqrt{2}}\left(|H_A H_B\rangle + e^{i\phi}\,|V_A V_B\rangle\right) \qquad (21)$$

with phase ϕ ($0 \leq \phi \leq \pi$) reliably controlled by micrometric displacements of M along $\mathbf{k}_p$. The phase stability, representing the most challenging experimental problem, has been solved by the use of the same back-mirror M for both wl's λ, λ_p In this way all the points symmetrically opposed through the center of the ring obtained by interception of the output cone with a plane orthogonal to $\mathbf{k}_p$, i.e. belonging to the so-called "entanglement-ring" (e-ring), are correlated by the same entanglement condition represented by the state $|\Phi\rangle$. An annular mask, with diameter $D = 2f \tan\xi = 15$ mm and width $\delta = 0.75$ mm, provides a very accurate spatial selection of the e-ring in the present experiment.

The degree of entanglement of the state generated by this source is characterized by the interference pattern in Figure 3a, corresponding to a coincidence visibility $V \geq 94\%$ over the entire emission cone. The dotted line corresponds to the limit boundary between the quantum and the classical regimes [12], while the theoretical continuous curve expresses the *ideal* interferometric pattern with maximum visibility: $V = 1$.

A positive lens ($f = 15$ cm) transforms the overall emission conical distribution into a cylindrical one with axis $\mathbf{k}_p$. The e-ring is divided in two equal portions along a vertical axis by a prism-like two-mirror system and directed to two independent measurement sites, $\mathcal{A}$ and $\mathcal{B}$ for polarization analysis and single photon detection. The detectors are silicon-avalanche mod.

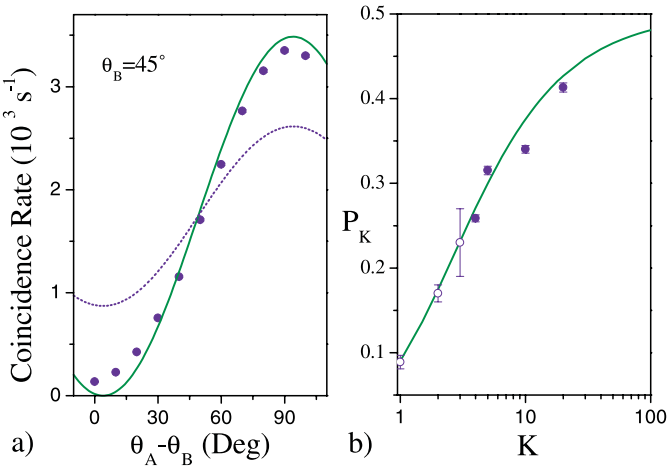

Fig. 3. (a) Measurement of the polarization entanglement for the state $|\Phi^-\rangle = (|H,H\rangle - |V,V\rangle)/\sqrt{2}$ obtained by varying the angle θ_A on site $\mathcal{A}$ in the range ($45°$–$135°$), having kept fixed the angle $\theta_B = 45°$ on site $\mathcal{B}$. (b) Plot of P_K against K. Black circles: experimental results for $K = 4, 5, 10, 20$ (error bars are lower than the dimensions of the corresponding experimental points). White circles: experimental results obtained in reference [7].

SPCM-AQR14 with quantum efficiency $QE = 65\%$ and dark count rate $\simeq$50 s^{-1}. Two equal interference filters, placed in front of the $\mathcal{A}$ and $\mathcal{B}$ with bandwidth $\Delta\lambda = 6$ nm, determined the coherence-time of the emitted photons: $\tau_{coh} \approx 140$ fs. More than 4×10^3 s^{-1} coincidences, corresponding to $\simeq 2 \times 10^5$ photon pairs emitted into collected modes, are measured at a pump power $P \simeq 100$ mW over the entire e-ring.

A zero-order $\lambda_p/4$ wp inserted between M and the BBO crystal, intercepting only the UV beam allows the engineering of tunable non maximally entangled states:

$$|\Phi\rangle = \alpha\,|H_A H_B\rangle + e^{i\phi}\beta\,|V_A V_B\rangle\,. \qquad (22)$$

By rotating the UV wp by an angle θ_p the polarization of the back-reflected pump beam is rotated by an angle $2\theta_p$ with respect to the optical axis of the crystal slab. Consequently, the emission efficiency of the $|H_A H_B\rangle$ contribution is lowered by a coefficient $\propto \cos^2 2\theta_p$. By adjusting θ_p in the range 0–$\pi/4$, γ can be continuously tuned between 1 and 0.

4 Experimental results

Demonstration of the violation of Hardy's inequality (20) requires the measurement of $2K + 2$ joint detection probabilities $P(\theta_A, \theta_B)$, where θ_A, θ_B are the angular settings of polarizers on sites $\mathcal{A}$ and $\mathcal{B}$ respectively (Fig. 2):

$$P_K = P(\theta_K, \theta_K) \leq P(\theta_0, \theta_0) + \sum_{k=1}^{K}\left[P(\theta_k, \theta_{k-1}^{\perp}) + P(\theta_{k-1}^{\perp}, \theta_k)\right] = \mathcal{P}, \qquad (23)$$

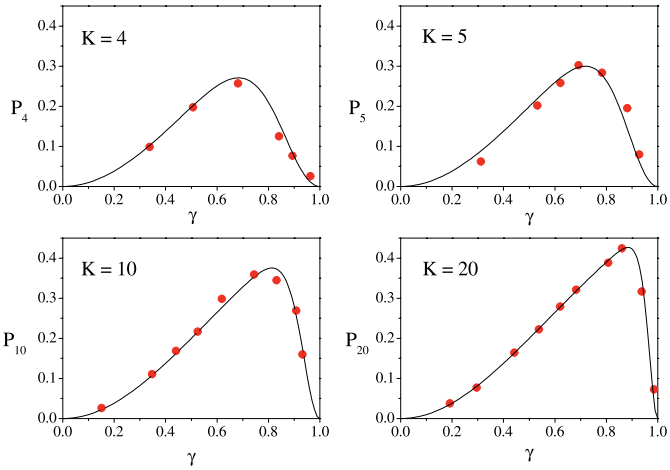

Fig. 4. Plots of P_4, P_5, P_{10}, P_{20} as a function of γ. The solid curves represent the theoretical predictions. The error bars are lower than the dimension of the corresponding experimental points.

with $\theta_k^{\perp} = \theta_k + \pi/2$. The experimental observation of inequality violation becomes more and more difficult as K increases because of an imperfect definition of the state and of the experimental uncertainties associated to the $2K + 2$ measurements. The above described source possess unique characteristics for this experiment because of the following reasons:

(1) it allows the direct generation of non maximally entangled states without postselection [7];
(2) its particular configuration of "single arm" interferometer guarantees a very high phase stability for long periods (>1 h);
(3) the high brightness allows to accumulate large sets of statistical data in a short measurement time ΔT.

By taking advantage of all these properties, we could successfully test Hardy's ladder theorem for large values of K. The experiment, realized for $K = 4$, 5, 10, 20 [13], has given the following violations of the inequality (23):

- $K = 4$ ($\Delta T = 60$ s): $P_4 = 0.2586 \pm 0.0041$; $\mathcal{P} = 0.1213 \pm 0.0022$. Inequality violated for 30σ;
- $K = 5$ ($\Delta T = 60$ s): $P_5 = 0.3152 \pm 0.0050$; $\mathcal{P} = 0.1184 \pm 0.0022$. Inequality violated for 37σ;
- $K = 10$ ($\Delta T = 120$ s): $P_{10} = 0.3402 \pm 0.0045$; $\mathcal{P} = 0.2288 \pm 0.0015$. Inequality violated for 26σ;
- $K = 20$ ($\Delta T = 180$ s): $P_{20} = 0.4132 \pm 0.0053$; $\mathcal{P} = 0.2439 \pm 0.0016$. Inequality violated for 21σ.

Each probability value has been obtained by normalizing the coincidence measurements to the sum of coincidence rates measured in the basis $|HH\rangle$ and $|VV\rangle$.

The count rates for each value of P_K are plotted in Figure 3b as a function of K. We report for comparison the results obtained in the experiment of reference [7]. The theoretical curve shown in the same figure indicates a very slow convergence to the asymptotic value $P_K = 0.5$. The experimental behavior of P_K as a function of γ, for $K = 4, 5, 10, 20$, are also plotted in Figure 4. The angle θ_K has been calculated for each value of γ by using the above given expression (18). The agreement of experimental data with theoretical predictions appears very good.

5 Towards a loophole-free nonlocality test

It is well-known that all nonlocality tests performed up to now in optics are affected by an efficiency loophole expressing the overall lack of detection of all couples of entangled photons [10,11]. Hence it can be concluded that the experimental results demonstrate the violation of local realism, only by taking on some supplementary assumptions. Concerning detection loophole, fair sampling hypothesis has to be introduced: the detected pairs are a characteristic subset of the whole set of generated pairs. It has been pointed out that, in order to observe a violation of local realism without any supplementary assumption, Clauser and Horne (CH) inequality has to be tested [3,10]:

$$\frac{P(\theta_A,\theta_B) - P(\theta_A,\theta'_B) + P(\theta'_A,\theta_B) + P(\theta'_A,\theta'_B)}{P(\theta'_A) + P(\theta_B)} \leq 1. \tag{24}$$

This expression is an inhomogeneous inequality, i.e. it involves both joint probabilities $P(\theta_A,\theta_B)$ and single count probabilities $P(\theta'_A)$. Quantum mechanics violates this inequality since it predicts a maximum value $(1+\sqrt{2})/2$ for the left member in the case of maximally entangled states.

In a typical SPDC-based experiment, the set of mode pairs coupled to the detectors are selected by a spatial filter, i.e. an iris diaphragm or an optical fiber, in order to realize particle detection over a single pair of correlated **k**-vectors [14]. Because of deviations from perfect phase matching, due to the inescapable effect of diffraction, it may happen that one photon passes through the spatial filter, while the correlated photon is intercepted. As a consequence, a state is obtained, which is given by the superposition of the polarization entangled pairs with single photon states, besides the vacuum field. In the common case of a coincidence experiment, the output state may be considered a post-selected two photon state. This post selection may cause conceptual difficulties when performing nonlocality tests [10].

In order to give a quantitative estimation of this effect, we can define a "correlation parameter", $g < 1$, as the conditional probability that photon B has not been intercepted, once photon A has passed through the spatial filter (and vice versa) [15]. A similar effect can be ascribed to any frequency filtering operation as well. By considering IF maximum transmittance, $T < 1$, and detector quantum efficiency, $\eta < 1$, the quantum mechanical limit for CH inequality is lowered by a factor $gT\eta$. It is worth noting that, in order to observe a violation of (24), it must be $gT\eta \geq 2/(1+\sqrt{2}) \simeq 0.83$. Typical values of T and η are $T \simeq 0.6$ for narrow bandwidth IF ($\Delta\lambda < 10$ nm), and $\eta \simeq 0.6$ for most commonly used silicon-avalanche detectors. These values don't allow to perform a loophole-free nonlocality measurement [10,11].

$$g = \left| \frac{\int d\mathbf{k}_A d\mathbf{k}_B \, f(\theta_A)\, f(\theta_B) F(\lambda_A) F(\lambda_B)\, \delta(\mathbf{k}_{A,\perp} + \mathbf{k}_{B,\perp})\, \delta(\omega_A + \omega_B - \omega_p)}{\int d\mathbf{k}_A d\mathbf{k}_B \, f(\theta_A)\, F(\lambda_A)\, \delta(\mathbf{k}_{A,\perp} + \mathbf{k}_{B,\perp})\, \delta(\omega_A + \omega_B - \omega_p)} \right|^2 \tag{29}$$

Large values of g can be attained by using wide spatial filters and IF filters with larger bandwidth. Indeed, the reduction of the filtering operations possesses a high conceptual relevance, because the original formulation of the EPR paradox necessarily concerns a purely quantum state, i.e. not affected by any "classical" manipulation. Frequency and **k**-vector filtering, instead, can be considered classical interventions on the emission process. The peculiar spatial properties of our source allow, at least in principle, to detect of the full set of optical modes without any spatial or λ-filtering, as said. This removal of filtering operation preserves the purity of the state, a condition long advocated by John Bell himself and never realized in practice [16].

We can evaluate the effects of wavelength and **k**-vector dispersion, by considering a SPDC process induced by a cw pump beam with Gaussian transverse profile propagating along the z-axis, through a thin crystal:

$$E_p(\mathbf{r}, t) = \mathcal{E}_p \exp\left[i(k_p\, z - \omega_p\, t)\right] \exp\left[-\left(\frac{\mathbf{r}_\perp}{\sigma}\right)^2\right]. \tag{25}$$

By SPDC two quantized fields are emitted from the crystal:

$$E_j^{(-)}(\mathbf{r}, t) = \int d\mathbf{k}_j \, d\omega_j \, \mathcal{E}_j \times \exp[-i(\mathbf{k}_j \cdot \mathbf{r} - \omega_j\, t)]\, a_j^\dagger(\mathbf{k}_j, \omega_j(\mathbf{k}_j)), \tag{26}$$

with $j = A,\ B$. In the low gain approximation, the two photon state can be written as [17]:

$$|\Psi\rangle = C \int d\mathbf{k}_A d\mathbf{k}_B \, \Phi(\mathbf{k}_A, \mathbf{k}_B) \times \delta(\omega_A + \omega_B - \omega_p) a_A^\dagger(\mathbf{k}_A) a_B^\dagger(\mathbf{k}_B)\, |0\rangle\,, \tag{27}$$

where the vacuum state has been omitted. In this expression we have

$$\begin{aligned} \Phi(\mathbf{k}_A, \mathbf{k}_B) &= \int_0^L dz \exp[-i(k_p - k_{s,z} - k_{i,z})z] \\ &\times \int d\mathbf{r}_\perp \exp\left[-\left(\frac{\mathbf{r}_\perp}{\sigma}\right)^2\right] \exp[-i(\mathbf{k}_{s,\perp} + \mathbf{k}_{i,\perp}) \cdot \mathbf{r}_\perp] \\ &\propto \operatorname{sinc}\frac{(k_p - k_{s,z} - k_{i,z})L}{2} \exp\left[-\frac{1}{4}\sigma^2(\mathbf{k}_{s,\perp} + \mathbf{k}_{i,\perp})^2\right], \end{aligned} \tag{28}$$

where L is the length of the crystal. The function $|\Phi(\mathbf{k}_A, \mathbf{k}_B)|^2$ accounts for deviations from the case of perfect phase matching condition, corresponding to a $L = \infty$ thick crystal pumped by a perfect plane wave. When using very thin crystals ($\lesssim$0.5 mm) transverse mismatch can be neglected with respect to the longitudinal effect, due to a limited value of L. In this way we can replace the Gaussian function in (28) with a Dirac delta function.

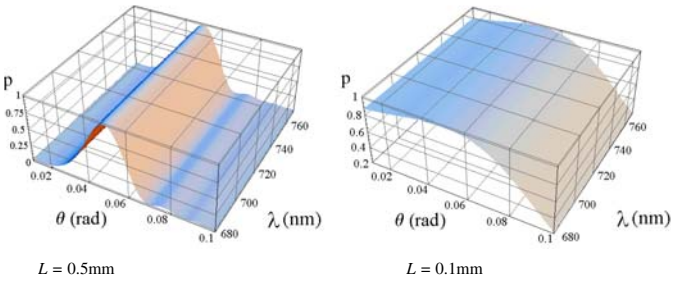

Fig. 5. Plot of the parametric emission probability p as a function of the wavelength λ and of the emission angle θ for two values of the crystal length L.

A three dimensional plot of the emission probability p, as a function of λ, in the range 680 nm $\leq \lambda \leq$ 760 nm and of the emission angle θ outside the crystal, in the horizontal plane, is shown in Figure 5 for $L = 0.5$ mm and $L = 0.1$ mm. While in the fist case p has a peak centered at $\theta \sim 50$ mrad, whose width is $\sim$20 mrad, almost independent on λ, in the second case the probability stays almost constant in the range $0 \leq \theta \leq 70$ mrad, then it vanishes very slowly.

By these considerations, in order to calculate the value of g, we can make two approximations: the first one is to consider p independent on θ and λ, i.e. to assume a uniform **k** and λ distribution. The second one is to consider only the effects of SPDC only on the horizontal plane. It is worth noting that for diaphragm apertures $\Delta\theta \gtrsim 20$ mrad, the dependence on λ can still be neglected, but the dependence on θ should be taken in account. However, the uniform **k** distribution approximation is still satisfactory for $L \leq 0.1$ mm, while it causes a lower estimation of the real value of g for $L = 0.5$ mm. Therefore, g can be expressed as

see equation (29) above

where $f(\theta)$ accounts for spatial filtering. We have $f(\theta) = 1$ when working well inside the spatial aperture $\Delta\theta$ and $f(\theta) = 0$ elsewhere. The function $F(\lambda_A)$ represents the shape of the frequency filters with maximum transmittance = 1.

Figure 6 shows the plot of g as a function of the spatial aperture $\Delta\theta$, calculated for different values of $\Delta\lambda$. Typical IF transmission functions can be approximated to a Gaussian shape in the case $\Delta\lambda = 6$ nm, and to a rectangular shape for $\Delta\lambda = 50$ nm, 100 nm. In the first case it comes out that the asymptotic value of g for large spatial apertures is $\simeq$0.5. The blue circle indicates the condition where the Hardy's ladder proof test described in this work has been performed: $g \simeq 0.45$. This number is further limited by the IF maximum transmittance T and the detector quantum efficiency η, as said. The main

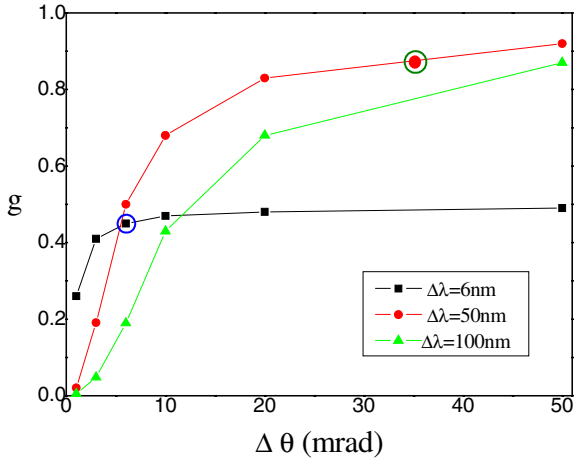

Fig. 6. Correlation parameter g as a function of the spatial aperture $\Delta\theta$, calculated for different values of the bandwidth $\Delta\lambda$ with maximum transmittance = 1. The blue circle indicates the ladder proof test condition of the present experiment; the green one indicates the numerical predictions for a test performed at $\Delta\lambda \sim 50$ nm and $\Delta\theta \lesssim 35$ mrad for $L = 0.1$ mm.

advantage of the mask is that it preserves the annular symmetry of the emission process, hence the number of single photon events is limited around the boundaries of the e-ring. In a typical experimental configuration (iris diaphragms of diameter ∼1 mm, aligned at ∼1 m far away from the crystal [14]) by this model we have $g \simeq 0.2$: however, this value represents an over-estimation of the real one, since the circular shape of the pinhole is not considered. This geometry, indeed, can not preserve the same value of correlation over the diaphragm surface.

In typical experimental conditions further limitations come out from critical dispersion effects due to photon transmission through birefringent media as BBO and the $\lambda/4$ wp and a relevant ϕ spread in states (21) is present. As a consequence, the larger the bandwidth $\Delta\lambda$, the lower the visibility of polarization interference fringes (Fig. 3a). In order to reduce this effect a nonlinear crystal slab and, possibly, a $\lambda/4$ wp as thin as possible should be adopted. Nonlinear crystals, 20 μm thick, are currently used for the measurement of ultrashort femtosecond pulses by autocorrelation techniques [18]. However these slabs are generally mounted on a fused silica substrate which causes unwanted dispersion. It seems reasonable to employ a 0.1 mm thick BBO crystal, which is thin enough to reduce dispersion, but does not require a substrate. Moreover, the presence of the $\lambda/4$ wp should be considered. An achromatic wp consists of two slabs of different birefringent materials (generally SiO_2 and MgF_2) with orthogonal optical axes [19]. By a suitable choice of the slabs thickness ($\leq$0.2 mm), it should be possible to keep the same phase shift between H and V components for a quite large bandwidth $\Delta\lambda$, while maintaining a still high fringes visibility. In this way, it seems reasonable to conceive an experimental set-up with limited dispersion effects over a wider bandwidth $\Delta\lambda$ with respect to the experiment described in the present paper. The choice of two IF with $\Delta\lambda \sim 50$ nm (a factor ∼9 larger than in the above described experiment) and of a mask aperture $\Delta\theta \lesssim 35$ mrad (a factor ∼7 larger than in the above described experiment) could allow to increase by a factor 2 the value of g (labelled by the green circle in Fig. 6).

Even if the realization of a perfect spatially correlated source (or at least a good approximation of it) does not mean to close the efficiency loophole until the detector efficiency will not be improved, this could represent a significant advancement towards an experiment, either involving an inequalities (Clauser-Horne) or without inequalities (Hardy), not requiring the adoption of supplementary assumptions.

6 Conclusions

We have presented an experimental test of quantum nonlocality realized by a high brilliance source of polarization entanglement. By virtue of the very large overall efficiency of the source, within the framework of the Hardy's ladder theory, a contradiction between standard quantum theory and local realism has been attained by for a fraction as large as 41% of the entangled photon pairs and as many as 20 steps of the ladder have been realized. An accurate discussion about the realization of an experimental test of quantum nonlocality with no need of supplementary assumptions has been given in the second part of the paper.

This work was supported by the FET European Network on Quantum Information and Communication (Contract IST-2000-29681: ATESIT), MIUR 2002-Cofinanziamento and PRA-INFM 2002 (CLON).

References

1. A. Einstein, B. Podolsky, N. Rosen, Phys. Rev. **47**, 777 (1935); J. Franklin Inst. **221**, 313 (1936)
2. J.S. Bell, Physics **1**, 165 (1964)
3. J.F. Clauser, M.A. Horne, A. Shimony, R.A. Holt, Phys. Rev. Lett. **23**, 880 (1969); J.F. Clauser, M.A. Horne, Phys. Rev. D **10**, 526 (1974)
4. A. Aspect, P. Grangier, G. Roger, Phys. Rev. Lett. **47**, 460 (1981); A. Aspect, P. Grangier, G. Roger, Phys. Rev. Lett. **49**, 91 (1982); A. Aspect, J. Dalibard, G. Roger, Phys. Rev. Lett. **47**, 1084 (1982)
5. E. Schroedinger, Proc. Camb. Phil. Soc. **31**, 555 (1935)
6. L. Hardy, Phys. Rev. Lett. **71**, 1665 (1993)
7. D. Boschi, S. Branca, F. De Martini, L. Hardy, Phys. Rev. Lett. **79**, 2755 (1997)
8. G. Giorgi, G. Di Nepi, P. Mataloni, F. De Martini, Laser Phys. **13**, 350 (2003); C. Cinelli, G. Di Nepi, F. De Martini, M. Barbieri, P. Mataloni, Phys. Rev. A **70**, 022321 (2004)
9. M. Barbieri, F. De Martini, G. Di Nepi, P. Mataloni, G.M. D'Ariano, C. Macchiavello, Phys. Rev. Lett. **91**, 227901 (2003); M. Barbieri, F. De Martini, G. Di Nepi, P. Mataloni, Phys. Rev. Lett. **92**, 177901 (2004)

10. E. Santos, Phys. Rev. Lett. **66**, 1388 (1991); E. Santos, Phys. Rev. A **46**, 3646 (1992); E. Santos, Phys. Lett. A **212**, 10 (1996)
11. N.D. Mermin, in *New Techniques and Ideas in Quantum Measurement* (The N.Y. Academy of Sciences, New York, 1986); A. Garuccio, Phys. Rev. A **52**, 2535 (1995); E.S. Fry, T. Walther, S. Li, Phys. Rev. A **52**, 4381 (1995)
12. S.Y. Ou, L. Mandel, Phys. Rev. Lett. **61**, 50 (1988)
13. M. Barbieri, F. De Martini, G. Di Nepi, P. Mataloni, preprint `arXiv:quant-ph/0406156`
14. P.G. Kwiat, K. Mattle, H. Weinfurter, A. Zeilinger, A.V. Sergienko, Y. Shih, Phys. Rev. Lett. **75**, 4337 (1995); C. Kurtsiefer, M. Oberparleiter, H. Weinfurther, Phys. Rev. A **64**, 023802 (2001). Note that, differently from our experiment and from other configurations (see e.g. P.G. Kwiat, E. Waks, A.G. White, I. Appelbaum, P.H. Eberhard, Phys. Rev. A **60**, R773 (1999)), in these works, type II phase matching crystals are employed. Polarization entanglement arises in this case by accurate spatial selection of only two correlated **k**-vectors
15. P. Grangier, private communication to FDM
16. A. Aspect, private communication to FDM; J. Bell, Comm. At. Mol. Phys. **9**, 121 (1980) reprinted in *Speakable and Unspeakable in QuantumMechanics* (Cambridge U. Press, 1987). There Aspect's experiment, in which no momentum correlation between entangled particles exists, was considered. In the case of SPDC tests, in which the spatial correlation is imposed by phase matching condition, the diffraction effects are determined by the finite thickness of the NL crystal and by the finite pump beam transverse profile
17. D. Klyshko, Photons and Nonlinear Optics (Gordon and Breach, New York, 1988)
18. M. Nisoli, S. De Silvestri, O. Svelto, R. Szipcs, K. Ferencz, Ch. Spielmann, S. Sartania, F. Krausz, Opt. Lett. **22**, 522 (1997)
19. See e.g.
`http://www.casix.com/product/Waveplate_WPA.htm;`
`http://www.cvilaser.com/static/tech_polartutor.asp`